
Boundary-Seeking Generative Adversarial Networks

R Devon Hjelm*
University of Montreal
Montreal Institute for Learning Algorithms
erroneus@gmail.com

Athul Paul Jacob*
University Of Waterloo
Montreal Institute for Learning Algorithms

Tong Che
University of Montreal
Montreal Institute for Learning Algorithms

Kyunghyun Cho
Courant Institute & Center for Data Science
New York University

Yoshua Bengio
University of Montreal
Montreal Institute for Learning Algorithms

Abstract

We introduce a novel approach to training generative adversarial networks (GANs, Goodfellow et al., 2014), where we train a generator to match a target distribution that converges to the data distribution at the limit of a perfect discriminator. This objective can be interpreted as training a generator to produce samples that lie on the decision boundary of the current discriminator in training at each update, and we call a GAN trained using this algorithm a boundary-seeking GAN (BGAN). This approach can be used to train a generator with discrete output when the generator outputs a parametric conditional distribution. We demonstrate the effectiveness of the proposed algorithm with discrete image and character-based natural language generation. Finally, we notice that the proposed boundary-seeking algorithm works even with continuous variables, and demonstrate its effectiveness with various natural image benchmarks.

1 Introduction

Generative adversarial networks (GAN, Goodfellow et al., 2014) involve a unique generative learning framework that uses two separate models with opposing, competing, or *adversarial* objectives. In contrast to those models that generate the data from a parametric distribution, such as directed graphical models (e.g., Helmholtz machines (Dayan et al., 1995) and variational autoencoders (VAEs, Kingma & Welling, 2013)) or undirected graphical models (e.g., restricted Boltzmann machines (RBMs, Hinton, 2002) and deep Boltzmann machines (DBMs, Salakhutdinov & Hinton, 2009)), GANs do not rely on maximum likelihood estimation (MLE, Dempster et al., 1977) to learn.

Rather, training a GAN, which consists of two competing networks—a discriminator and a generator—only requires back-propagating a learning signal originating from a learned objective function corresponding to the loss of a discriminator trained in an adversarial way. This framework is powerful, as it trains a generator without relying on an explicit formulation of the probability function which requires marginalizing out latent variables. Also, it avoids the issue with the MLE objective which makes an MLE-trained model conservative in probability mass placement. The latter issue is known to be a problem behind MLE-trained models generating samples that lack real-world qualities, often evidenced by the lack of sharpness in natural images (Goodfellow, 2016). Unlike MLE-trained

* Authors contributed equally.

models, GANs have been shown to generate often-diverse and realistic samples even when trained on high-dimensional large-scale data (Radford et al., 2015) in the case of continuous variables.

GANs however have a serious limitation on the type of variables they can model, because they require the composition of the generator and discriminator to be fully differentiable. With discrete variables, this is not true. For instance, consider using a step function at the end of a generator in order to generate a discrete value. In this case, back-propagation alone cannot provide the training signal for the generator, because the derivative of a step function is 0 almost everywhere (and so would be the back-propagated signal). This is problematic, as many important real-world datasets are discrete, such as character- or word-based representations of language. The general issue of credit assignment for computational graphs with discrete operations (e.g. discrete stochastic neurons) is difficult, and only approximate solutions have been proposed in the past (Bengio et al., 2013; Gu et al., 2015; Gumbel & Lieblein, 1954; Jang et al., 2016; Maddison et al., 2016; Tucker et al., 2017).

In this paper, we introduce a novel learning algorithm for GANs. This algorithm estimates the gradient of the discriminator’s output w.r.t. the generator as the weighted sum of the gradients of the log-probabilities of the samples generated from the generator. The weights are given by the discriminator’s performance on the samples, such that those samples that look similar to true training examples, are weighted more (because they would be scored highly by the discriminator). This lets us interpret the discriminator as computing a target distribution for the discrete stochastic units, allowing us to train a generator to converge toward the hypothetical true distribution of the data as the discriminator is optimized. This objective can further be interpreted as an alternative loss on the discriminator output, which allows us to derive a novel learning algorithm for GANs even with continuous variables. Under this interpretation, the learning objective of a generator is to minimize the difference between the discriminator’s log-probabilities for the sample being positive and negative. This objective can be thought of as training the generator to *place generated samples at the decision boundary of the discriminator*, and hence we call a GAN trained with the proposed algorithm a boundary-seeking generative adversarial network (BGAN).

We demonstrate the effectiveness of the proposed BGAN in both settings, with discrete as well as continuous variables. We use MNIST and quantized CelebA for the discrete image setting, and street view house numbers (SVHN, Netzer et al., 2011), CIFAR-10 (Krizhevsky & Hinton, 2009), CelebA (Liu et al., 2015), and the Caltech-USCB birds dataset (Welinder et al., 2010) for the continuous image setting. We compare to competing GAN objectives using the CelebA dataset. We also demonstrate discrete BGAN on a simple character-based model on the 1-billion word dataset (Chelba et al., 2013), showing successful learning and stability for natural language generation. In the case of continuous variables, we observe that the proposed algorithm works qualitatively better than conventional GANs.

2 Methods

2.1 Generative Adversarial Networks

The generative adversarial networks (GAN, Goodfellow et al., 2014) framework combines two models: a generator model pitted against a discriminatory adversary. The generator is composed of a prior distribution, $p(\mathbf{z})$, over latent variable \mathbf{z} and a generator function, $G(\mathbf{z})$, which maps from the space of \mathbf{z} to the space of data \mathbf{x} . The objective of the discriminator is to correctly distinguish between data and samples from the generator by maximizing

$$\mathbb{E}[\log D(\mathbf{x})]_{\mathbf{x} \sim p_{\text{data}}(\mathbf{x})} + \mathbb{E}[\log(1 - D(G(\mathbf{z})))]_{\mathbf{z} \sim p(\mathbf{z})}, \quad (1)$$

where $D(\cdot)$ is a discriminator function with output that spans $[0, 1]$. The generator is trained to “fool” the discriminator, that is minimize $\mathbb{E}[\log(1 - D(G(\mathbf{z})))]_{\mathbf{z} \sim p(\mathbf{z})}$ or to minimize a proxy $\mathbb{E}[-\log(D(G(\mathbf{z})))]_{\mathbf{z} \sim p(\mathbf{z})}$. Ignoring the proxy case, the two models play a minimax game with value function:

$$\min_G \max_D V(G, D) = \mathbb{E}[\log D(\mathbf{x})]_{\mathbf{x} \sim p(\mathbf{x})} + \mathbb{E}[\log(1 - D(G(\mathbf{z})))]_{\mathbf{z} \sim p(\mathbf{z})}. \quad (2)$$

The GAN generator is defined by the composition of sampling the latent values \mathbf{z} and applying the deterministic function G . The generative objective involves one continuous function with param-

ters from both models: $D(G(\cdot; \psi); \phi)$, but optimized over ϕ only. This allows for training a generative model with a relatively simple fitness function and back-propagation, rather than a complex marginalized likelihood function, and which does not suffer from some of the learning difficulties of maximum likelihood estimators (MLE), e.g., giving rise to blurred samples.

In practice, the generator, rather than being trained to minimize the above value function, can be trained to maximize the proxy $\log(D(G(\mathbf{z})))$ or $\log(D(G(\mathbf{z}))) - \log(1 - D(G(\mathbf{z})))$, which can alleviate some learning issues related to the discriminator loss saturating early in learning and improve stability. In addition, recent advances using mean-squared error (LSGAN, Mao et al., 2016) or the earth-movers distance (WGAN, Arjovsky et al., 2017) as alternative learning signals for both the discriminator and generator can improve the approach.

In order for a generating function, $G(\cdot; \psi)$, with real-valued parameters, ψ , to generate discrete-valued outputs, \mathbf{x} , $G(\cdot; \psi)$ cannot be fully continuous. A natural choice for the generator would be a continuous function, $\mathbf{y} = f(\mathbf{z})$ (e.g., a feed forward network), followed by a step function. However, as the gradients that would otherwise be used to train the generator are zero almost everywhere, it is not possible to train the generator from the discriminator error signal. Approximations for the back-propagated signal exist (Bengio et al., 2013; Gu et al., 2015; Gumbel & Lieblein, 1954; Jang et al., 2016; Maddison et al., 2016; Tucker et al., 2017). We propose a novel approach to dealing with this issue, based on estimating a proposal target distribution for the generator output.

2.2 Target distribution for the generator

First consider the optimal discriminator function (Goodfellow et al., 2014), $D(\mathbf{x})^*$, derived from analytically optimizing the discriminator objective given a fixed generator $G(\cdot)$ and assuming no functional constraints on the discriminator, i.e., in a non-parametric setting:

$$D_G^*(\mathbf{x}) = \frac{p_{\text{data}}(\mathbf{x})}{p_{\text{data}}(\mathbf{x}) + p_g(\mathbf{x})}, \quad (3)$$

where $p_{\text{data}}(\mathbf{x})$ is the data distribution, and $p_g(\mathbf{x})$ is the distribution as generated by $p(\mathbf{z})$ and $G(\mathbf{z})$. Given this optimal discriminator, the density of the data can then be written as:

$$p_{\text{data}}(\mathbf{x}) = p_g(\mathbf{x}) \frac{D_G^*(\mathbf{x})}{1 - D_G^*(\mathbf{x})}. \quad (4)$$

This indicates that, in the limit of a perfect discriminator, the true distribution can be perfectly estimated from a said discriminator and any fixed generator, even if that generator is not perfectly trained. *A sample from that corrected estimator can thus be obtained by reweighing samples from the generator according to the ratio $\frac{D_G^*(\mathbf{x})}{1 - D_G^*(\mathbf{x})}$.* Unfortunately, it is unlikely that such a perfect discriminator is learnable or even exists. However, one can posit the following estimator for the true distribution, given an imperfect discriminator, $D(\mathbf{x})$:

$$\tilde{p}(\mathbf{x}) = \frac{1}{Z} p_g(\mathbf{x}) \frac{D(\mathbf{x})}{1 - D(\mathbf{x})}, \quad \text{where } Z = \sum_{\mathbf{x}} p_g(\mathbf{x}) \frac{D(\mathbf{x})}{1 - D(\mathbf{x})} \quad (5)$$

is the normalization constant that guarantees that $\tilde{p}(\mathbf{x})$ is a proper probability distribution. This distribution was discovered independently from us by Che et al. (2017). Note that the optimum for the generator occurs at $D(\mathbf{x}) = D^*(\mathbf{x}) = 1/2$, so that $Z = 1$ and $\tilde{p}(\mathbf{x}) = p_g(\mathbf{x}) = p(\mathbf{x})$. $\tilde{p}(\mathbf{x})$ is a potentially biased estimator for the true density; however, *the bias only depends on the quality of $D(\mathbf{x})$: the closer $D(\mathbf{x})$ is to $D^*(\mathbf{x})$, the lower the bias.* This is an important consideration because it is likely that training the discriminator (a standard probabilistic binary classifier) is much easier than training the generator (whose objective function is a moving target as the discriminator adapts to the generator and vice-versa). The optimum for the generator exists when generated samples have equal probability of being classified as data or as samples. This occurs at the decision boundary of the discriminator, so that we call this approach boundary-seeking generative adversarial networks (BGAN).

2.3 BGAN with discrete variables

For discrete variables, parameterizing the generating distribution directly reveals a method for training the generator without relying on back-propagation through the generator’s discrete output. As

with previous work on evaluating GANs (Wu et al., 2016), we parameterize $p_g(\mathbf{x})$ as the marginalization of a joint density, $p_g(\mathbf{x}) = \sum_{\mathbf{z}} g(\mathbf{x}|\mathbf{z})p(\mathbf{z})$, rephrasing the generator function, $G(\mathbf{z})$, as a conditional distribution, $g(\mathbf{x}|\mathbf{z})$. To minimize the distance between $\tilde{p}(\mathbf{x})$ and $p_g(\mathbf{x})$, we can minimize the exclusive KL divergence, so that the gradients w.r.t. the generator parameters, ψ , are (the full derivation can be found in the Appendix):

$$\nabla_{\psi} D_{KL}(\tilde{p}(\mathbf{x})||p_g(\mathbf{x})) = -\frac{1}{Z} \mathbb{E} \left[\sum_{\mathbf{x}} g(\mathbf{x}|\mathbf{z}) \frac{D(\mathbf{x})}{1-D(\mathbf{x})} \nabla_{\psi} \log p_g(\mathbf{x}) \right]_{\mathbf{z} \sim p(\mathbf{z})}, \quad (6)$$

where $\tilde{p}(\mathbf{x})$ is held fixed. Note that, while $\tilde{p}(\mathbf{x})$ depends on the generator parameters, ψ , we interpret this distribution as the current estimate of the true density and hence a *target* for the generator. The gradients would require some sort of Monte-Carlo (MC) estimator across the input and output noise, and will have high variance, notably due to the partition function, Z . The intuition here is to note that, as the conditional density, $g(\mathbf{x}|\mathbf{z})$, is unimodal, it can be used to define a low-variance estimator analogous to that of Equation 5. Following this intuition and by inspection of Eq. 6, we propose updating the joint distribution, $p(\mathbf{x}, \mathbf{z}) = g(\mathbf{x}|\mathbf{z})p(\mathbf{z})$, to fit the joint target distribution:

$$\tilde{p}(\mathbf{x}, \mathbf{z}) = \tilde{p}(\mathbf{x}|\mathbf{z})p(\mathbf{z}) = \frac{1}{Z_{|\mathbf{z}}} g(\mathbf{x}|\mathbf{z}) \frac{D(\mathbf{x})}{1-D(\mathbf{x})} p(\mathbf{z}), \quad (7)$$

where $\tilde{p}(\mathbf{x}|\mathbf{z})$ is an estimate of the data in the neighborhood of the generated samples defined by \mathbf{z} and $Z_{|\mathbf{z}} = \sum_{\mathbf{x}} g(\mathbf{x}|\mathbf{z}) \frac{D(\mathbf{x})}{1-D(\mathbf{x})}$ is the partition function that ensures $\tilde{p}(\mathbf{x}|\mathbf{z})$ is a proper probability distribution. Note we are no longer targeting marginal of Equation 5, as the marginal of the joint given by Equation 7 over \mathbf{z} , which is also normalized, has the same convergence behavior as Equation 5. The gradients then can be estimated as the exclusive KL divergence of the joint distributions:

$$\begin{aligned} \nabla_{\psi} D_{KL}(\tilde{p}(\mathbf{x}, \mathbf{z})||p_g(\mathbf{x}, \mathbf{z})) &\approx -\mathbb{E} [\tilde{p}(\mathbf{x}|\mathbf{z}) \nabla_{\psi} \log g(\mathbf{x}|\mathbf{z})]_{\mathbf{z} \sim p(\mathbf{z})} \\ &= -\mathbb{E} \left[\frac{1}{Z_{|\mathbf{z}}} \sum_{\mathbf{x}} g(\mathbf{x}|\mathbf{z}) \frac{D(\mathbf{x})}{1-D(\mathbf{x})} \nabla_{\psi} \log g(\mathbf{x}|\mathbf{z}) \right]_{\mathbf{z} \sim p(\mathbf{z})} \approx -\mathbb{E} \left[\sum_m \tilde{w}^{(m)} \nabla_{\psi} \log g(\mathbf{x}^{(m)}|\mathbf{z}) \right]_{\mathbf{z} \sim p(\mathbf{z})}, \end{aligned}$$

$$\text{where } \tilde{w}^{(m)} = \frac{w^{(m)}}{\sum_{m'} w^{(m')}} \quad \text{and} \quad w^{(m)} = \frac{D(\mathbf{x}^{(m)})}{1-D(\mathbf{x}^{(m)})}$$

are the normalized and unnormalized importance weights respectively (note how $Z_{|\mathbf{z}}$ cancels in the normalization) and $\mathbf{x}^{(m)}$ are samples from the generator for the given \mathbf{z} . The normalization can help generate a relative learning signal, which will help in the case that the samples are all fairly bad from the point of view of $D(\mathbf{x})$. The benefit of using Equation 7 over Equation 5 is clear: the normalized weights, $\tilde{w}^{(m)}$, when $\mathbf{x}^{(m)}$ is sampled from a unimodal distribution, will be of low variance compared to those estimated by marginalizing over \mathbf{z} . The gradients can be computed over a mini-batch of samples from $p(\mathbf{z})$, which reveals a straightforward procedure for training discrete GANs with a parametric conditional generator without relying on back-propagation. Compared to normal GANs, this method requires M times more space, but computing the M (instead of 1) scalar values of $D(\mathbf{x}^{(m)})$ can be parallelized, as samples from $g(\mathbf{x}|\mathbf{z})$ can be drawn independently.

One could have derived a similar learning objective using the *inclusive* KL divergence (rather than the exclusive in our formulation), so that the gradients become (see Appendix for details):

$$\nabla_{\psi} D_{KL}(p_g(\mathbf{x}, \mathbf{z})||\tilde{p}(\mathbf{x}, \mathbf{z})) \approx -\mathbb{E} \left[\frac{1}{M} \sum_m (\log w^{(m)} - \log Z_{|\mathbf{z}} - 1) \nabla \log g(\mathbf{x}^{(m)}|\mathbf{z}) \right]_{\mathbf{z} \sim p(\mathbf{z})}. \quad (8)$$

This gradient strongly resembles REINFORCE, and in fact we can interpret $\log Z_{|\mathbf{z}}$ as an input-dependent baseline (using a deep neural network trained with MSE to predict $\log Z_{|\mathbf{z}}$, using \mathbf{z} as input), as in neural variational inference and learning (NVIL, Mnih & Gregor, 2014).

2.4 Continuous variables

While we originally set out to find a means for training discrete GANs, the insight above can also be used to provide a learning algorithm in the continuous case. For continuous variables, we could introduce a parametric conditional distribution (such as Gaussian) as we did in the discrete case,

defining importance weights, and computing a gradient directly at the generator output using the KL divergence. However, this would abandon some of the strengths central to GANs relative to other generative models with continuous data (Goodfellow, 2016).

While a tractable form of $p_g(\mathbf{x})$ is unavailable to us, a simple analysis of Equation 5 shows that the distance (by a number of metrics) between $\tilde{p}(\mathbf{x})$ and $p_g(\mathbf{x})$ is minimized when $\frac{1}{Z} \frac{D(\mathbf{x})}{1-D(\mathbf{x})} = 1$. This indicates an alternative learning objective to training GANs for a generator of continuous data. There are a number of loss functions that would be suitable, and we have experimented with a simple squared-error loss:

$$\mathcal{L}_g(\mathbf{x}) = (\log D(\mathbf{x}) - \log(1 - D(\mathbf{x})) - \log Z)^2. \quad (9)$$

An alternative is to use the cross-entropy with a target of $1/2$ (this has been done in the context of domain adaptations, e.g., Tzeng et al., 2015), though the above loss works very well in practice. In the case of discriminators with a simple sigmoid output, $D(\mathbf{x}) = \sigma(r(\mathbf{x}))$, where $\sigma(r) = \frac{1}{1+e^{-r}}$, the loss simplifies to:

$$\mathcal{L}_g(\mathbf{x}) = (r(\mathbf{x}) - \log Z)^2. \quad (10)$$

As the ratio $\frac{D(\mathbf{x})}{1-D(\mathbf{x})}$ converges to one, so does the partition function, which can be used to formulate an alternative objective to Equation 10, but without the $\log Z$ term. Though this also works in practice, in our experiments using an estimate of $\log Z$ can improve stability and results. When used, we estimate $\log Z$ using a moving average of Monte-Carlo estimates for each update, t :

$$\log \tilde{Z}_{t+1} = \gamma \log \tilde{Z}_t + (1 - \gamma) \frac{1}{N} \log \left(\sum_n \frac{D(\mathbf{x}_t^{(n)})}{1 - D(\mathbf{x}_t^{(n)})} \right), \quad (11)$$

where γ is hyper-parameter controlling the moving average, and $\mathbf{x}_t^{(n)}$ are the batch of N generated samples at the t -th step.

While the continuous-case loss has a very different form from that of the discrete cases, the optimum is the same and corresponds exactly with the minimum of the KL divergence. The above loss function can be used as an alternative to the usual GAN generator objective for continuous data, and we demonstrate its effectiveness in our experiments below.

3 Related Work

GAN for discrete variables Our approach introduces new learning algorithms that allows for training generative adversarial networks (GANs) on discrete data. Discrete data with GANs is an active and unsolved area of research, particularly with language model data involving recurrent neural network (RNN) generators (Yu et al., 2016; Li et al., 2017). Our importance sampling-based solution is analogous to reweighted wake-sleep (RWS, Bornschein & Bengio, 2014), a successful approach for training Helmholtz machines with discrete variables (but not in a GAN framework).

Other REINFORCE-based methods have been proposed for language modeling (Yu et al., 2016; Che et al., 2017), but the solution we introduce is derived from the inclusive KL divergence following directly from the intuition of BGAN. The REINFORCE estimator works, though less well compared to the importance sampling-based BGAN in our experiments of the following section. This situation is analogous to performance of RWS vs NVIL in sigmoid belief networks (SBMs), where RWS outperforms the input-dependent baseline method. Alternatively, advanced techniques (Mnih & Rezende, 2016) may improve the REINFORCE-based method, though we leave this for future work.

The Gumbel-Softmax technique is another approach to train Helmholtz machines with discrete variables (Jang et al., 2016; Maddison et al., 2016), which effectively allows for training them as variational autoencoders (VAEs, Kingma & Welling, 2013). However, this technique has only been shown to work in very limited settings, and has yet to been shown to work well with GANs with discrete data. In our experiments, we find that this estimator does not help train GANs, and these results can be found in the Appendix. More recent approaches, such as REBAR Tucker et al. (2017), may prove to be more successful, but this is left for future work.

Learning algorithms for GAN Since its introduction by Goodfellow et al. (2014), there have been a number of novel objectives for improving GAN training. Recently, Arjovsky et al. (2017), proposed a modification to the learning procedure of GAN based on the earth-mover’s distance. This method works very well for stabilizing GAN training, but necessarily limits the capacity of the discriminator to limit its Lipschitz constant. Mao et al. (2016) proposed a mean-squared error-based approach that improves mode coverage. Our work contributes to this pile of recent works, however, with a distinct goal of building a unified learning framework for both discrete and continuous variables. In addition, LSGAN shares the same optimal discriminator as BGAN in the form of Equation 3. This indicates an alternative learning objective for the generator in LSGANs, such that the target lies at the average of the real and fake targets of the discriminator (e.g., $1/2$ in a 0-1 coding). Finally, traditional GANs rely on the generator pushing the generated samples in the direction of highest certainty as “true” data, or towards infinity in the logit space. This causes the well-known pathology of GANs sometimes pushing the samples beyond the true samples, thus causing learning to fail. This pathology is explicitly absent from the GAN objective, which removes one possible source of instability (see Appendix for more details).

Implicit inference There is a strong connection to implicit variational inference with GANs (Tran et al., 2017; Huszár, 2017), where the logit of a binary GAN (r in Equation 10) can be used as a proxy for the log-ratio in the variational lower bound. This indicates an alternative approach to encoder / decoder type GANs (Dumoulin et al., 2016), so that the objective is to ensure that the encoding and decoding distributions match. This is left for future work.

4 Discrete variables

4.1 Datasets and setup

We first test our approach to training discrete generative adversarial networks (GANs) using two imaging benchmarks: the common discretized MNIST dataset (Salakhutdinov & Murray, 2008) and a new quantized version of the CelebA dataset (see Liu et al., 2015, for the original CelebA dataset). For CelebA quantization, we first downsampled the images from 64×64 to 32×32 . We then generated a 16-color palette using Pillow, a fork of the Python Imaging Project (<https://python-pillow.org>). This palette was then used to quantize the RGB values of the CelebA samples to a one-hot representation of 16 colors. Next, we test BGAN with natural language generation with the 1-billion word dataset (Chelba et al., 2013) at the character-level, limiting the dataset to sentences of at least and truncating to 32 characters. As we found better results with the importance-weighted version of BGAN, we use this version for discrete data unless otherwise noted. Our implementation for discrete BGAN as well as the continuous case in the next Section can be found at <https://github.com/rdevon/BGAN>.

For imaging data, our models used deep convolutional GANs (DCGAN, Radford et al., 2015). The generator is fed a vector of 64 i.i.d. random variables drawn from a uniform distribution, $[0, 1]$. The output nonlinearity was sigmoid for MNIST to model the Bernoulli centers $g(x_i|\mathbf{z})$ for each pixel, while the output was softmax for quantized CelebA. For character-level language generation, we follow recent work with advanced training of WGANs (Gulrajani et al., 2017), and use deep CNNs for both the generator and discriminator. For the input-dependent baseline REINFORCE method in Equation 8, we use a three layer fully-connected neural network with 256 hidden units, leaky-ReLU units, and batch normalization (BN, Ioffe & Szegedy, 2015). We applied BN to the generator, as is consistent in the literature. However, across our experiments with discrete datasets, we found that BN in the discriminator made for unstable learning and worse results. We therefore omitted the BN from the discriminator.

The model was trained using the Adam method for stochastic optimization (Kingma & Ba, 2014) with exponential decay rates of $\beta_1 = 0.95$ and $\beta_2 = 0.5$. MNIST was trained for 100 epochs, while quantized CelebA was trained for 50 epochs. Unlike what is commonly done in the literature for training GANs (Goodfellow et al., 2014; Arjovsky et al., 2017), the discriminator was not updated multiple times for every generator update. We trained the model with learning rates of $1e-4$, $1e-5$, and $1e-6$ to test convergence properties. The number of samples per generated examples, M , was set to 20, which was used to generate the normalized weights and train the input-dependent baseline.



Figure 1: Left: Random samples from the generator trained as a boundary-seeking GAN (BGAN) with discrete MNIST data. Shown are the Bernoulli centers of the generator conditional distribution. Samples show high variability, with realistic generated hand-drawn digits.

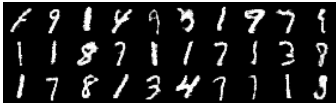


Figure 2: Left: Random samples from the generator trained using the REINFORCE-like algorithm with an input-dependent baseling. Samples are of good quality, but the model is missing modes.



Figure 3: Left: Ground-truth 16-color (4-bit) quantized CelebA images downsampled to 32×32 . Right: Samples produced from the generator trained as a boundary-seeking GAN on the quantized CelebA for 50 epochs.

Table 1: Random samples drawn from a generator trained with the discrete BGAN objective. The model is able to successfully learn many important character-level English language patterns.

And it 's miant a quert could he	He weirst placed produces hopesi	What 's word your changerg bette
" We pair of condels of money wi	Sance Jory Chorotic , Sen doesin	In Lep Edger 's begins of a find",
Lankard Avaloma was Mr. Palin ,	What was like one of the July 2	" I stroke like we all call on a
There says the sounded Sunday in	The BBC nothing overton and slea	With there was a passes ipposing
About dose and warthestrinds fro	College is out in contesting rev	And tear he jumped by even a roy

4.2 Generation result

Our results showed that training the importance-weighted BGAN on discrete MNIST data is stable and produces realistic and highly variable generated handwritten digits. Figure 1 shows example digits from the model trained with a learning rate of $1e-4$, sampled randomly from the generator to demonstrate individual digit quality, respectively. The model was relatively robust against learning rate, showing stable learning for the generator across learning rates tested without any noticeable sensitivity to hyperparameters. For quantized CelebA, the generator trained as a BGAN produced reasonably realistic images, which resemble the original dataset well. In addition, the faces produced are highly variable, and show the type of diversity we expect from a good generator.

For language data, training with BGAN yielded stable, reliably good character-level generation (Table 1), though generation is poor compared to recurrent neural network-based methods (Sutskever et al., 2011; Mikolov, 2012). We are however not aware of any previous work in which a discrete GAN, without any continuous relaxation (Gulrajani et al., 2017), was successfully trained from scratch without any pretraining and without any auxiliary supervised loss to generate any sensible text. Despite the low quality of the text relative to the existing supervised recurrent language model, we find it a favourable evidence showing the stability and capability of the proposed boundary-seeking criterion for training discrete GAN.

5 Continuous Variables

5.1 Datasets and setup

We tested the boundary-seeking objective on street view house numbers (SVHN Netzer et al., 2011), CIFAR-10 (Krizhevsky & Hinton, 2009), CelebA, and the Caltech-USCB birds dataset (Welinder et al., 2010, scaled to 64×64). As with our experiments with discrete data, we used the DCGAN architecture. We used this same parameterization, except with one additional convolutional layer for both the generator and discriminator, as is consistent with the literature. We also used 100 i.i.d. random variables for the 64×64 image datasets and 64 variables for the 32×32 image datasets, each drawn from a uniform distribution. All models were trained with the same Adam hyper-parameters and a learning rate of $1e-3$.

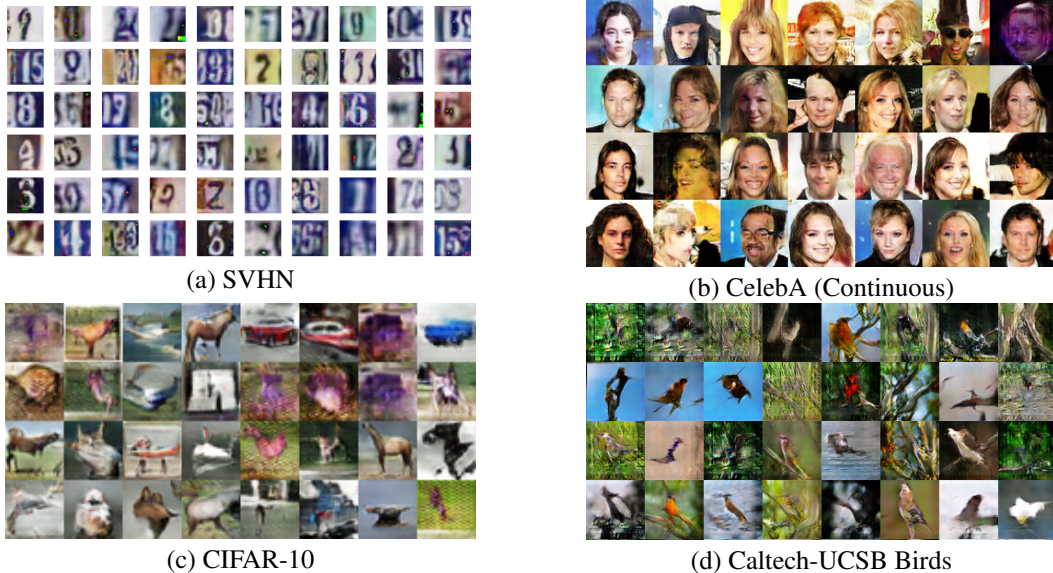


Figure 4: Samples generated from the continuous BGANs trained on various real-valued benchmark datasets; (a) SVHN (32x32), (b) CelebA (64x64 without quantization), (c) CIFAR-10 (32x32), and (d) rescaled Caltech-USBC Birds dataset (64x6x). Both SVHN and CIFAR-10 were generated from BGAN trained setting $\log Z = 0$, while CelebA and Caltech-UCSB birds were generated using the moving average in Equation 11.

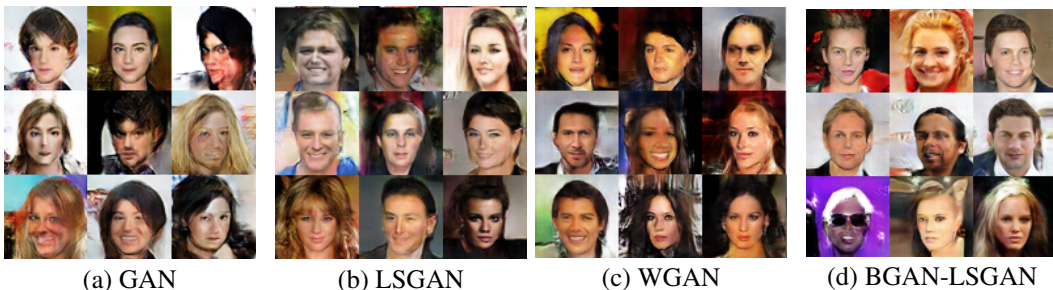


Figure 5: Examples generated from other GAN objectives with the same architecture; (a) GAN, (b) LSGAN, (c) WGAN, and (d) LSGAN trained with a boundary-seeking objective, setting the generator target to $1/2$.

For the 32x32 CIFAR-10 and SVHN datasets, BGAN setting $\log Z = 0$ was sufficient. For the larger 64x64 images from CelebA and Caltech-UCSB birds, we found that estimating $\log Z$ from Equation 11 improved stability and achieved better samples.

Next, we used CelebA to compare between various GAN variants: normal GAN, least-squares GAN (LSGAN Mao et al., 2016), and Wasserstein GAN (WGAN Arjovsky et al., 2017). In addition, we train on a boundary-seeking version of LSGANs, setting the generator target to $1/2$ with a 0-1 coding discriminator. We tested on a wider range learning rates and selected those for which the models performed the best qualitatively. Although Arjovsky et al. (2017) recommends otherwise, we trained all models, including WGAN, with one discriminator update per generator update, as in the context of our initial experiments we found there to be no discernible difference. All models were trained for a maximum of 30 epochs, though models were stopped early in the case of collapse.

5.2 Generation result

Example generations from BGAN are presented in Figure 4 (Full sets can be found in the Appendix). Of all of the models shown, only normal GANs collapsed within the number of epochs run, so we show the last best samples for normal GANs. BGAN performs well generating images from the imaging datasets and performs comparably in image quality to that of LSGANs and WGANs (Figure 5), but better than normal GANs within the constraints of our hyperparameter search and

training procedures. Surprisingly, LSGAN with the $1/2$ generator target performs very well, generating samples that are at least of equal quality to WGAN, BGAN, and LSGAN.

Though we found that BGAN with continuous data did not easily collapse, it did so more than WGAN, which seems relatively robust against collapse in our experiments (though WGAN can produce strong artifacts or be slow to train, depending on the hyper-parameters). Particularly for larger datasets like CelebA, we found that BGAN performed better with higher learning rates ($1e-3$), higher “leaking” on the discriminator rectifier nonlinearities, and at least 2 discriminator updates per generator update during learning. However, none of the models we tested were absolutely reliable in image quality across a wide range of learning rates, and we conclude that BGAN can produce high-dimensional images as well as WGAN and LSGAN.

6 Conclusion

Reinterpreting the generator objective to match the proposal target distribution reveals a novel learning algorithm for training a generative adversarial network (GANs, Goodfellow et al., 2014). This proposed approach of boundary-seeking provides us with a unified framework under which learning algorithms for both discrete and continuous variables are derived. Empirically, we showed the effectiveness of training a GAN with the proposed learning algorithm, to which we refer as a boundary-seeking GAN (BGAN), on both discrete and continuous variables.

Acknowledgements

RDH thanks IVADO, MILA, UdeM, NIH grants R01EB006841 and P20GM103472, and NSF grant 1539067 for support. APJ thanks UWaterloo, Waterloo AI lab and MILA for their support and Michael Noukhovitch, Pascal Poupart for constructive discussions. KC thanks TenCent, eBay, Google (Reward Awards 2015, 2016), NVIDIA (NVAIL) and Facebook for their support. YB thanks CIFAR, NSERC, IBM, Google, Facebook and Microsoft for their support. Finally, we wish to thank the developers of Theano (Al-Rfou et al., 2016), Lasagne <http://lasagne.readthedocs.io>, and Fuel (Van Merriënboer et al., 2015) for their valuable code-base.

References

- Al-Rfou, Rami, Alain, Guillaume, Almahairi, Amjad, Angermueller, Christof, Bahdanau, Dzmitry, Ballas, Nicolas, Bastien, Frédéric, Bayer, Justin, Belikov, Anatoly, et al. Theano: A python framework for fast computation of mathematical expressions. *arXiv preprint arXiv:1605.02688*, 2016.
- Arjovsky, Martin, Chintala, Soumith, and Bottou, Léon. Wasserstein gan. *arXiv preprint arXiv:1701.07875*, 2017.
- Bengio, Yoshua, Léonard, Nicholas, and Courville, Aaron. Estimating or propagating gradients through stochastic neurons for conditional computation. *arXiv preprint arXiv:1308.3432*, 2013.
- Bornschein, Jörg and Bengio, Yoshua. Reweighted wake-sleep. *arXiv preprint arXiv:1406.2751*, 2014.
- Che, Tong, Li, Yanran, Zhang, Ruixiang, Hjelm, R Devon, Li, Weijie, Song, Yangqiu, and Bengio, Yoshua. Maximum-likelihood augmented discrete generative adversarial networks. *arXiv preprint*, 2017.
- Chelba, Ciprian, Mikolov, Tomas, Schuster, Mike, Ge, Qi, Brants, Thorsten, Koehn, Phillipp, and Robinson, Tony. One billion word benchmark for measuring progress in statistical language modeling. *arXiv preprint arXiv:1312.3005*, 2013.
- Dayan, Peter, Hinton, Geoffrey E, Neal, Radford M, and Zemel, Richard S. The helmholtz machine. *Neural computation*, 7(5):889–904, 1995.
- Dempster, Arthur P, Laird, Nan M, and Rubin, Donald B. Maximum likelihood from incomplete data via the em algorithm. *Journal of the royal statistical society. Series B (methodological)*, pp. 1–38, 1977.

- Dumoulin, Vincent, Belghazi, Ishmael, Poole, Ben, Lamb, Alex, Arjovsky, Martin, Mastropietro, Olivier, and Courville, Aaron. Adversarially learned inference. *arXiv preprint arXiv:1606.00704*, 2016.
- Goodfellow, Ian. Nips 2016 tutorial: Generative adversarial networks. *arXiv preprint arXiv:1701.00160*, 2016.
- Goodfellow, Ian, Pouget-Abadie, Jean, Mirza, Mehdi, Xu, Bing, Warde-Farley, David, Ozair, Sherryl, Courville, Aaron, and Bengio, Yoshua. Generative adversarial nets. In *Advances in Neural Information Processing Systems*, pp. 2672–2680, 2014.
- Gu, Shixiang, Levine, Sergey, Sutskever, Ilya, and Mnih, Andriy. Muprop: Unbiased backpropagation for stochastic neural networks. *arXiv preprint arXiv:1511.05176*, 2015.
- Gulrajani, Ishaan, Ahmed, Faruk, Arjovsky, Martin, Dumoulin, Vincent, and Courville, Aaron. Improved training of wasserstein gans. *arXiv preprint arXiv:1704.00028*, 2017.
- Gumbel, Emil Julius and Lieblein, Julius. Statistical theory of extreme values and some practical applications: a series of lectures. *US Govt. Print. Office*, 1954.
- Hinton, Geoffrey E. Training products of experts by minimizing contrastive divergence. *Neural computation*, 14(8):1771–1800, 2002.
- Huszár, Ferenc. Variational inference using implicit distributions. *arXiv preprint arXiv:1702.08235*, 2017.
- Ioffe, Sergey and Szegedy, Christian. Batch normalization: Accelerating deep network training by reducing internal covariate shift. *arXiv preprint arXiv:1502.03167*, 2015.
- Jang, Eric, Gu, Shixiang, and Poole, Ben. Categorical reparameterization with gumbel-softmax. *arXiv preprint arXiv:1611.01144*, 2016.
- Kingma, Diederik and Welling, Max. Auto-encoding variational bayes. *arXiv preprint arXiv:1312.6114*, 2013.
- Kingma, DP and Ba, J. Adam: A method for stochastic optimization. *arXiv preprint arXiv:1412.6980*, 2014.
- Krizhevsky, Alex and Hinton, Geoffrey. Learning multiple layers of features from tiny images. *Citeseer*, 2009.
- Li, Jiwei, Monroe, Will, Shi, Tianlin, Ritter, Alan, and Jurafsky, Dan. Adversarial learning for neural dialogue generation. *arXiv preprint arXiv:1701.06547*, 2017.
- Liu, Ziwei, Luo, Ping, Wang, Xiaogang, and Tang, Xiaoou. Deep learning face attributes in the wild. In *Proceedings of the IEEE International Conference on Computer Vision*, pp. 3730–3738, 2015.
- Maddison, Chris J, Mnih, Andriy, and Teh, Yee Whye. The concrete distribution: A continuous relaxation of discrete random variables. *arXiv preprint arXiv:1611.00712*, 2016.
- Mao, Xudong, Li, Qing, Xie, Haoran, Lau, Raymond YK, Wang, Zhen, and Smolley, Stephen Paul. Least squares generative adversarial networks. *arXiv preprint ArXiv:1611.04076*, 2016.
- Mikolov, Tomáš. *Statistical Language Models Based on Neural Networks*. PhD thesis, Ph. D. thesis, Brno University of Technology, 2012.
- Mnih, Andriy and Gregor, Karol. Neural variational inference and learning in belief networks. In *Proceedings of the 31st International Conference on Machine Learning (ICML-14)*, pp. 1791–1799, 2014.
- Mnih, Andriy and Rezende, Danilo J. Variational inference for monte carlo objectives. *arXiv preprint arXiv:1602.06725*, 2016.
- Netzer, Yuval, Wang, Tao, Coates, Adam, Bissacco, Alessandro, Wu, Bo, and Ng, Andrew Y. Reading digits in natural images with unsupervised feature learning. In *NIPS workshop on deep learning and unsupervised feature learning*, volume 2011, pp. 5, 2011.
- Radford, Alec, Metz, Luke, and Chintala, Soumith. Unsupervised representation learning with deep convolutional generative adversarial networks. *arXiv preprint arXiv:1511.06434*, 2015.
- Salakhutdinov, Ruslan and Hinton, Geoffrey E. Deep boltzmann machines. In *International Conference on Artificial Intelligence and Statistics*, pp. 448–455, 2009.

- Salakhutdinov, Ruslan and Murray, Iain. On the quantitative analysis of deep belief networks. In *Proceedings of the 25th international conference on Machine learning*, pp. 872–879. ACM, 2008.
- Sutskever, Ilya, Martens, James, and Hinton, Geoffrey E. Generating text with recurrent neural networks. In *Proceedings of the 28th International Conference on Machine Learning (ICML-11)*, pp. 1017–1024, 2011.
- Tran, Dustin, Ranganath, Rajesh, and Blei, David M. Deep and hierarchical implicit models. *arXiv preprint arXiv:1702.08896*, 2017.
- Tucker, George, Mnih, Andriy, Maddison, Chris J, and Sohl-Dickstein, Jascha. Rebar: Low-variance, unbiased gradient estimates for discrete latent variable models. *arXiv preprint arXiv:1703.07370*, 2017.
- Tzeng, Eric, Hoffman, Judy, Darrell, Trevor, and Saenko, Kate. Simultaneous deep transfer across domains and tasks. In *Proceedings of the IEEE International Conference on Computer Vision*, pp. 4068–4076, 2015.
- Van Merriënboer, Bart, Bahdanau, Dzmitry, Dumoulin, Vincent, Serdyuk, Dmitriy, Warde-Farley, David, Chorowski, Jan, and Bengio, Yoshua. Blocks and fuel: Frameworks for deep learning. *arXiv preprint arXiv:1506.00619*, 2015.
- Welinder, P., Branson, S., Mita, T., Wah, C., Schroff, F., Belongie, S., and Perona, P. Caltech-UCSD Birds 200. Technical Report CNS-TR-2010-001, California Institute of Technology, 2010.
- Wu, Yuhuai, Burda, Yuri, Salakhutdinov, Ruslan, and Grosse, Roger. On the quantitative analysis of decoder-based generative models. *arXiv preprint arXiv:1611.04273*, 2016.
- Yu, Lantao, Zhang, Weinan, Wang, Jun, and Yu, Yong. Seqgan: sequence generative adversarial nets with policy gradient. *arXiv preprint arXiv:1609.05473*, 2016.

7 Appendix

7.1 Derivation of importance-weighted discrete BGAN

Here we derive the gradient of the exclusive KL divergence between the joint target distribution, $\tilde{p}(\mathbf{x}, \mathbf{z})$, which is kept fixed w.r.t. the generative parameters, ψ , and the joint generator distribution, $p_g(\mathbf{x}, \mathbf{z}) = g(\mathbf{x}|\mathbf{z})p(\mathbf{z})$.

$$\begin{aligned}
\nabla_{\psi} D_{KL}(\tilde{p}(\mathbf{x})||p_g(\mathbf{x})) &= \nabla_{\psi} \sum_{\mathbf{x}} \tilde{p}(\mathbf{x}) \log \frac{\tilde{p}(\mathbf{x})}{p_g(\mathbf{x})} \\
&= - \sum_{\mathbf{x}} \tilde{p}(\mathbf{x}) \nabla_{\psi} \log p_g(\mathbf{x}) = - \sum_{\mathbf{x}} \frac{1}{Z} p_g(\mathbf{x}) \frac{D(\mathbf{x})}{1 - D(\mathbf{x})} \nabla_{\psi} \log p_g(\mathbf{x}) \\
&= - \sum_{\mathbf{x}} \sum_{\mathbf{z}} \frac{1}{Z} g(\mathbf{x}|\mathbf{z}) p(\mathbf{z}) \frac{D(\mathbf{x})}{1 - D(\mathbf{x})} \nabla_{\psi} \log p_g(\mathbf{x}), \tag{12}
\end{aligned}$$

7.2 REINFORCE-based algorithm

Here we derive the REINFORCE-based algorithm from the inclusive KL divergence between the joint target distribution and the joint generation distribution.

$$\begin{aligned}
\nabla_{\psi} D_{KL}(p_g(\mathbf{x}, \mathbf{z}) || \tilde{p}(\mathbf{x}, \mathbf{z})) &= \nabla_{\psi} \sum_{\mathbf{x}, \mathbf{z}} p(\mathbf{z}) g(\mathbf{x}|\mathbf{z}) \log \frac{p_g(\mathbf{x}, \mathbf{z})}{\tilde{p}(\mathbf{x}, \mathbf{z})} \\
&= \sum_{\mathbf{x}, \mathbf{z}} p(\mathbf{z}) \left(\nabla_{\psi} g(\mathbf{x}|\mathbf{z}) \log \frac{p_g(\mathbf{x}, \mathbf{z})}{\tilde{p}(\mathbf{x}, \mathbf{z})} + g(\mathbf{x}|\mathbf{z}) \nabla_{\psi} \log p_g(\mathbf{x}, \mathbf{z}) \right) \\
&= \sum_{\mathbf{x}, \mathbf{z}} p(\mathbf{z}) \left(\nabla_{\psi} g(\mathbf{x}|\mathbf{z}) (\log g(\mathbf{x}|\mathbf{z}') - \log \tilde{p}(\mathbf{x}|\mathbf{z})) + g(\mathbf{x}|\mathbf{z}) \nabla_{\psi} \log p(\mathbf{z}) g(\mathbf{x}|\mathbf{z}) \right) \\
&= \sum_{\mathbf{x}, \mathbf{z}} p(\mathbf{z}) g(\mathbf{x}|\mathbf{z}) \left(\nabla_{\psi} \log g(\mathbf{x}|\mathbf{z}) (\log g(\mathbf{x}|\mathbf{z}) - \log \tilde{p}(\mathbf{x}|\mathbf{z})) + \nabla_{\psi} \log g(\mathbf{x}|\mathbf{z}) \right) \\
&= - \sum_{\mathbf{x}, \mathbf{z}} p(\mathbf{z}) g(\mathbf{x}|\mathbf{z}) \nabla_{\psi} \log g(\mathbf{x}|\mathbf{z}) \left(\log \frac{D(\mathbf{x})}{1 - D(\mathbf{x})} - \log Z_{|\mathbf{z}|} + 1 \right) \\
&\approx - \mathbb{E} \left[\frac{1}{M} \sum_m \left(\log w^{(m)} - \log Z_{|\mathbf{z}|} - 1 \right) \nabla \log g(\mathbf{x}^{(m)} | \mathbf{z}^{(n)}) \right]_{\mathbf{z} \sim p(\mathbf{z})}. \tag{13}
\end{aligned}$$

The log-partition function can be estimated a number of ways. The simplest is to estimate using a logarithm of the Monte-Carlo estimate:

$$\log Z_{|\mathbf{z}|} = \log \sum_{\mathbf{x}} g(\mathbf{x}|\mathbf{z}) \frac{D(\mathbf{x})}{1 - D(\mathbf{x})} \approx \log \sum_m \frac{D(\mathbf{x}^{(m)})}{1 - D(\mathbf{x}^{(m)})} - \log M, \tag{14}$$

where $\mathbf{x}^{(m)} \sim g(\mathbf{x}|\mathbf{z})$ are M samples drawn from the generator given \mathbf{z} . To reduce variance, we can use a moving average, as in Equation 11. However, these estimates do not capture the dependence of \mathbf{z} . As in Mnih & Gregor (2014), we can use an input-dependent baseline with parameters ϕ , $C(\mathbf{z}; \phi)$, using a neural network with input \mathbf{z} . This network is trained with the simple MSE loss function:

$$\mathcal{L}_{\phi} = \mathbb{E} \left[C(\mathbf{z}; \phi) - \log \sum_m \frac{D(\mathbf{x}^{(m)})}{1 - D(\mathbf{x}^{(m)})} + \log M \right]_{\mathbf{z} \sim p(\mathbf{z})}^2. \tag{15}$$

7.3 Visual comparison: GAN vs. BGAN

In the case of continuous variables, we can qualitatively analyze the difference between the conventional GAN and the proposed boundary-seeking GAN. We consider an one-dimensional variable, and draw 20 samples as each of real and generated sets of samples from two Gaussian distributions. We consider two cases; (a) early stage of learning, and (b) late stage of learning. We use -2 and 2 in the first case, and -0.1 and 0.1 in the second case, for the centers of those two Gaussians. The variances were set to 0.3 for both distributions. Instead of learning, we simply set our discriminator $D(x)$ to

$$D(x) = \frac{1}{1 + \exp(-cx)},$$

where c is set to 0.8 and 10 for the cases (a) and (b), respectively. These values were selected to illustrate sub-optimal discriminators, which is almost always true when training a GAN on a real data.

In Fig. 6, we plot both real and generated samples on the x-axis ($y = 0$). The solid red curve corresponds to the discriminator $D(x)$ above, and its log-gradient ($\partial \log D(x) / \partial x$) is drawn with a dashed red curve. It is clear that maximizing $\log D(x)$, as conventionally done with GAN, pushes the generator beyond the real samples (orange circles). On the other hand, the proposed criterion from Eq. (9) has its minimum at the decision boundary of the discriminator. Minimizing this criterion has the effect of pushing the generated samples, or correspondingly the generator, toward the

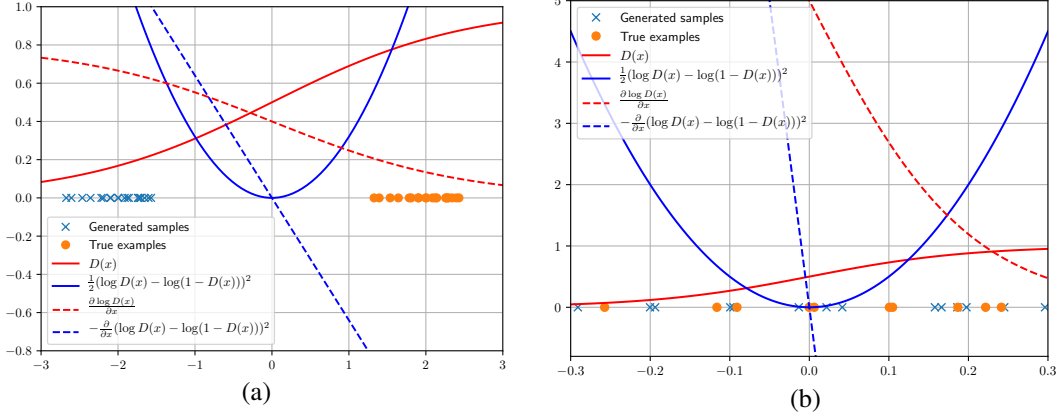


Figure 6: Qualitative comparison between the conventional GAN and the proposed BGAN in 1-D examples. The discriminator D is fixed to a logistic regression classifier with a coefficient 0.8. Note that the maximum of the generator objective from the conventional GAN is at the positive infinity (red curve), while the minimum from the proposed BGAN is at the decision boundary (blue curve). Unlike the proposed BGAN, the learning gradient of the conventional GAN (red dashed curve) pushes the generated samples beyond the real samples.

real samples, but never beyond the region occupied by them. The issue is much more apparent in Fig. 6 (b), where the real and generated samples are extremely close to each other. The proposed BGAN encourages the generator to stay close to the center of real samples, while the conventional objective pushes the generated samples beyond the real samples. We conjecture that this property avoids a well-known failure mode of GANs and improves learning.

7.4 Training discrete GANs with Gumbel softmax

Table 2: Hyperparameters used in our sweep of discrete GANs trained using the Gumbel-Softmax and straight-through Gumbel-Softmax

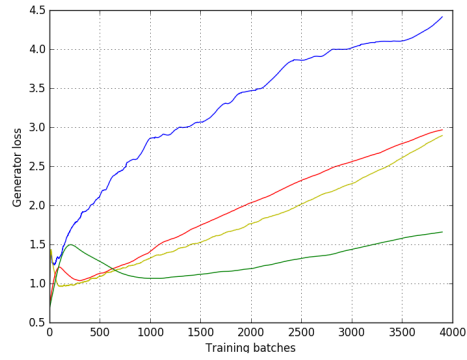
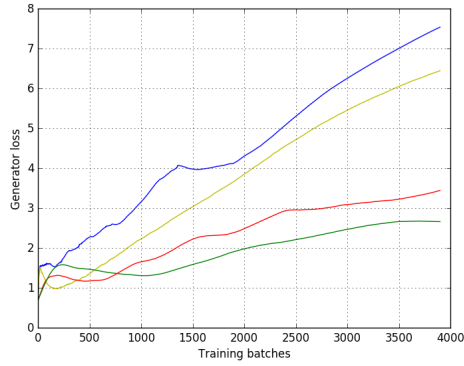
Optimizer	[Adam, RMSProp, SGD]
Learning Rate	[$1e-2$, $1e-3$, $1e-4$, $1e-5$]
Anneal Rate (r)	[0.01, 0.001, 0.0001]
Anneal Interval (N)	[200, 300, 500]

The "Gumbel technique" (Gumbel & Lieblein, 1954; Jang et al., 2016) has been shown to be successful in some tasks where back-propagation through discrete random variables is not possible. Using the same model parameterization as our MNIST experiments above, we compare our approach to Gumbel-Softmax (Maddison et al., 2016; Jang et al., 2016) and straight-through Gumbel-Softmax (Maddison et al., 2016; Jang et al., 2016) on the binarized MNIST dataset. The temperature was annealed using the schedule $\tau = \max(0.5, \exp(-rt))$ as a function of the global training step t , where τ is updated every N steps. The values for the grid search of r and N are listed in Table 2.

We observed that the generator cost of Gumbel-Softmax and straight-through Gumbel diverged across all hyperparameters (Figure 7). No set of hyperparameters produced a generator that was able to produce satisfactory representative samples of the original dataset.

7.5 Generation results

Provided are the complete set of random samples, which were truncated in the main text.



(a)

(b)

Gumbel-Softmax

		b	y	r	g
(a)	lr	adam	rmsprop	adam	rmsprop
	r	10^{-4}	10^{-4}	10^{-5}	10^{-5}
	N	10^{-3}	10^{-4}	10^{-3}	10^{-3}
(b)	lr	adam	rmsprop	adam	rmsprop
	r	10^{-4}	10^{-4}	10^{-5}	10^{-5}
	N	10^{-3}	10^{-5}	10^{-3}	10^{-3}

Gumbel-Softmax (Straight-Through)

Figure 7: The diverging behaviour of the generator training when using Gumbel-Softmax technique, both (a) with and (b) without straight-through estimation. The curves are a running average and are sampled from our hyperparameter search:



(a) SVHN



(b) CelebA (Continuous)



(c) CIFAR-10

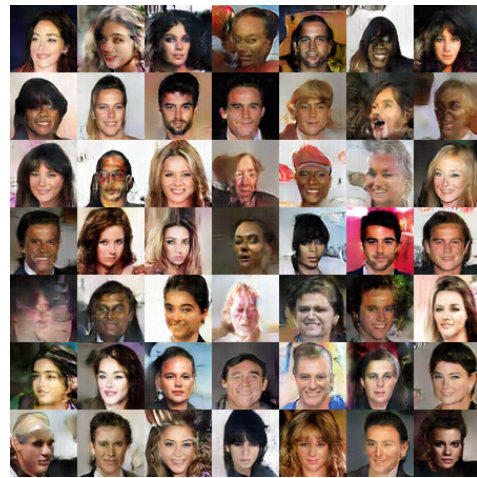


(d) Caltech-UCSB Birds

Figure 8: Samples generated from the continuous BGANs trained on various real-valued benchmark datasets; (a) SVHN (32x32), (b) CelebA (64x64 without quantization), (c) CIFAR-10 (32x32), and (d) rescaled Caltech-USBC Birds dataset (64x64).



(a) GAN



(b) LSGAN



(c) WGAN



(d) BGAN-LSGAN

Figure 9: Examples generated from other GAN objectives with the same architecture; (a) GAN $lr=1e-4$, (b) LSGAN $lr=1e-3$, (c) WGAN $lr=1e-4$, and (d) LSGAN trained with a boundary-seeking objective, setting the generator target to $1/2$, $lr=1e-3$.